Aalborg Universitet

AALBORG UNIVERSITY
DENMARK

Effect of dopants in polyaniline-coated capacitive deionization electrodes on anion selectivity

Gamaethiralalage, J. G.; Muff, Jens; de Smet, Louis C.P.M.

Published in:
Progress in Organic Coatings

DOI (link to publication from Publisher):
10.1016/j.porgcoat.2024.108854

Creative Commons License
CC BY 4.0

Publication date:
2024

Document Version
Publisher's PDF, also known as Version of record

Link to publication from Aalborg University

Citation for published version (APA):
Gamaethiralalage, J. G., Muff, J., & de Smet, L. C. P. M. (2024). Effect of dopants in polyaniline-coated capacitive deionization electrodes on anion selectivity. *Progress in Organic Coatings*, *197*, Article 108854. https://doi.org/10.1016/j.porgcoat.2024.108854

General rights
Copyright and moral rights for the publications made accessible in the public portal are retained by the authors and/or other copyright owners and it is a condition of accessing publications that users recognise and abide by the legal requirements associated with these rights.

- Users may download and print one copy of any publication from the public portal for the purpose of private study or research.
- You may not further distribute the material or use it for any profit-making activity or commercial gain
- You may freely distribute the URL identifying the publication in the public portal -

Take down policy
If you believe that this document breaches copyright please contact us at vbn@aub.aau.dk providing details, and we will remove access to the work immediately and investigate your claim.

Progress in Organic Coatings 197 (2024) 108854

Contents lists available at ScienceDirect

Progress in Organic Coatings

journal homepage: www.elsevier.com/locate/porgcoat

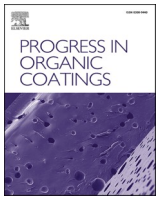

Effect of dopants in polyaniline-coated capacitive deionization electrodes on anion selectivity

J.G. Gamaethiralalage [a,b], Jens Muff [b], Louis C.P.M. de Smet [a,*]

[a] Laboratory of Organic Chemistry, Wageningen University, Stippeneng 4, 6708 WE Wageningen, The Netherlands
[b] Department of Chemistry & Bioscience, Aalborg University, Niels Bohrs Vej 8, 6700 Esbjerg, Denmark

ARTICLE INFO

Keywords:
Polyaniline
Electrodeposition
Dopants
Activated carbon
Capacitive deionization
Ion separation

ABSTRACT

This study explores the viability of employing polyaniline (PAni) coatings doped with different anions in capacitive deionization (CDI) electrodes for ion recovery purposes. Multiple CDI electrodes were fabricated by electrodepositing PAni in the presence of four mineral acids (HCl, HNO_3, H_2SO_4, and H_3PO_4) to incorporate the corresponding anions into the PAni network. The results highlight the critical role of dopants and polymerization conditions in determining ion adsorption behavior. Notably, the PAni/H_2SO_4 electrode achieved approximately 20 % reduction in chloride adsorption while maintaining consistent sulfate adsorption compared to the control. The behavior of PAni/HCl, PAni/HNO_3, and PAni/H_3PO_4 systems were not as pronounced compared to the PAni/H_2SO_4 system, under tested parameters, highlighting the dopant-dependent influence of polymerization conditions. Specifically focusing on the PAni/H_2SO_4 system, various polymerization conditions were investigated, and their ion adsorption characteristics were evaluated using a CDI system. It was observed that reducing the monomer concentration or the polymerization duration can enhance the selective properties of the coated electrode in this specific scenario. Additionally, distinct differences in polymer morphology based on polymerization conditions and dopants were observed, underlining the need for further research to understand the influence of these variables on the morphology of the PAni network and the resulting ion adsorption behavior of the coatings.

1. Introduction

In recent years, capacitive deionization (CDI), an electrochemical desalination method, has made notable advances in resource recovery [1]. CDI removes ions from aqueous media by adsorbing charged species onto porous electrodes under an applied potential or a current, forming an electrical double layer. The applications and theory of CDI is well reviewed in literature [2–6]. Ion selectivity in CDI can be enhanced through varied electrode materials, ion-exchange membranes, optimized operational parameters, and functionalized electrodes or membranes.

Ion selectivity is crucial for sensing and extracting different ionic species in aqueous systems. Common methods to achieve ion selectivity include membrane filtration, biofiltration, chemical precipitation, sorbent materials, and electrochemical separation. In applications such as water treatment and resource recovery, selectivity challenges often emerge, particularly with valuable species like phosphates and nitrates.

In the early 1970s, molecularly imprinted polymers (MIPs) were introduced to address ion selectivity challenges in organic compounds [7,8]. MIPs are created by synthesizing polymers with a template, which is later removed, leaving specific binding sites for target compounds, mimicking biological host-guest interactions. Shortly after, ion-imprinted polymers (IIPs) were developed by Nishide et al. [9], using ligand complexes with metal ions to form selective binding sites. While MIPs rely on hydrogen bonding and Van der Waals forces, IIPs operate on metal-ligand complexes. Recently, the use of MIPs and IIPs has grown in separation and sensor applications, offering insights for improving inorganic ion selectivity.

In the context of CDI, functionalizing porous carbon materials has emerged as a promising strategy to enhance ion selectivity and improve electrode properties such as capacity and transfer kinetics. Recently, integrating conducting polymers into CDI electrodes has gained significant attention [10]. It is important to note that early studies in this field placed a predominant emphasis on enhancing the capacity of CDI electrodes rather than focusing on achieving selective ion separation. Among the conducting polymers, polypyrrole and polyaniline are the

* Corresponding author.
E-mail address: louis.desmet@wur.nl (L.C.P.M. de Smet).

https://doi.org/10.1016/j.porgcoat.2024.108854
Received 8 July 2024; Received in revised form 20 September 2024; Accepted 4 October 2024
Available online 18 October 2024
0300-9440/© 2024 The Authors. Published by Elsevier B.V. This is an open access article under the CC BY license (http://creativecommons.org/licenses/by/4.0/).

most widely used for these applications [11].

The use of conducting polymers in CDI for selective ion recovery is a recent advancement. Ji et al. [12] reported an ion-exchange hybrid film of bismuth oxychloride/chloride ion-imprinted polypyrrole for selective chloride removal. Han et al. [13] developed a lithium-selective electrode using dibenzo-14-crown-4, multi-walled carbon nanotubes, and polypyrrole, where polypyrrole acted as a conducting agent rather than the selective component. Wang et al. [14] introduced an asymmetric CDI system with Mxene/carbon nanofiber composite electrodes, one doped with chloride-modified polypyrrole and the other with dodecylbenzenesulfonate-modified polypyrrole, to selectively remove divalent ions (calcium and magnesium) over monovalent ions (sodium and potassium).

Polyaniline (PAni) [15] is one of the most extensively studied conducting polymers [16,17]. The preparation [18–20], structure [21–24], dopants [25,26], and electrochemical behavior [27], of PAni has been explored thoroughly. Wu et al. [28] demonstrated selective fluoride ion removal using a polyaniline-carbon nanotube composite, increasing selectivity towards fluoride from 0.26 to 1.22. Zornitta et al. [29] reported polyaniline activated carbon modified with polyaniline for chloride selectivity over phosphate and sulfate, while Gao et al. [30] investigated ferrocene-polyaniline functionalized carbon nanotubes for phosphate selectivity over chloride, nitrate, and sulfate. Li et al. [31] developed a polyaniline-derived mesoporous carbon flow-electrode system selective for ammonium ions over calcium and magnesium. These studies highlight PAni's potential in selective ion separation. PAni can be synthesized chemically, using ammonium persulfate (APS) as an oxidant and dopant [18], or electrochemically, where the monomer is directly oxidized at the anode. The latter ensures doping with the desired anion from the mineral acid used.

Building on our previous work [29], this study aims to explore the behavior of polyaniline on activated carbon electrodes when polymerized in the presence of different mineral acids. While existing literature often focuses on using a single dopant in conducting polymers for CDI electrodes, the impact of varying dopants on selective ion adsorption has been largely overlooked. Polyaniline's "memory effect," where the polymer retains the dopant size memory, was first studied over two decades ago by Lapkowski et al. [32] for its impact on electroactivity. This work seeks to leverage this effect to improve the selective ion separation of CDI electrodes. In this study, aniline is electropolymerized on commercially available activated carbon electrodes using HCl, HNO_3, H_2SO_4, and H_3PO_4 as acidic media. The goal is to assess the feasibility of enhancing ion selectivity in CDI electrodes through this method.

2. Materials and methods

2.1. Materials

Sodium chloride (NaCl, >99 %) was purchased from Alfa Aesar. Sodium phosphate monobasic (NaH_2PO_4, ≥99 %), phosphoric acid (H_3PO_4, ≥85 % wt in H_2O), sodium sulfate (Na_2SO_4, ≥99 %) were obtained from Sigma-Aldrich. Sodium nitrate ($NaNO_3$, >99 %) was purchased from VWR chemicals. Hydrochloric acid (HCl, 37 % wt in H_2O) was acquired from Supelco. Sulfuric acid (H_2SO_4, 95–98 % wt in H_2O) and nitric acid (HNO_3, 70 % wt in H_2O) were obtained from Honeywell Fluka. All chemicals were reagent grade and used as received without any further purification. Aniline (99 %, Sigma-Aldrich) was distilled using a vacuum distillation setup to remove any impurities, dimers, and oligomers and stored in the refrigerator in airtight containers until further use. Selemion CMVN cation-exchange membranes were purchased from AGC Engineering, Japan. The activated carbon electrodes used as working electrodes were provided by Voltea BV, The Netherlands. Carbon cloth used as counter electrodes in the CDI system was purchased from Kynol, Germany. Autolab PGSTAT 302N, PGSTAT 128N (Metrohm BV, The Netherlands) and Origaflex OGF05A (Origalys, France) potentiostats were used to run all experiments. The samples were analyzed via ion chromatography with an ECO IC (Metrohm BV, The Netherlands), equipped with either a Metrosep A Supp 19-100/4.0 or Metrosep A Supp 10-100/2.0 column, running on a carbonate/bicarbonate eluent system, and calibrated with standards made in house (0–100 ppm range of chloride, sulfate, nitrate, and phosphate). The samples were injected with an 863 Compact IC autosampler (Metrohm BV).

2.2. Methods

2.2.1. Electropolymerization

For electropolymerization of aniline, a three-electrode electrochemical cell was used. A 10 cm × 2 cm piece of activated carbon electrode, an Ag/AgCl (3 M KCl) electrode, and an oversized activated carbon electrode were used as working, reference, and counter electrodes, respectively. Polymerization was carried out using a potentiodynamic method by sweeping the potential in a −0.2 V to 0.7 V window at a scan rate of 1 mV/s, for 60 cycles. The polymerization solution consisted of 1 M of the mineral acid (HCl, HNO_3, H_2SO_4, or H_3PO_4) and 0.1 M of the distilled aniline monomer in 250 mL. The electrodes were placed inside a 3D-printed electrode holder to prevent accidental short circuiting during polymerization. These electrodes are henceforth referred to as PAni/HCl, PAni/HNO_3, PAni/H_2SO_4, and PAni/H_3PO_4, respectively. After the polymerization step, the electrodes were rinsed with the respective mineral acid to remove any dimers or oligomers on the surface, and then with DI water. The electrodes were then stored in DI water until further use.

Additionally, electrodeposition involved the utilization of a potentiostatic method. In this approach, a constant potential of 0.9 V was applied to the working electrode, employing the same three-electrode cell as previously described. Variations in monomer concentration and polymerization duration were introduced to examine their impact on desalination performance. The focus of this investigation was on the PAni/H_2SO_4 system, with adjustments made to electrodeposition parameters. Following this protocol, promising parameters were extended to other PAni systems. In a separate phase, an electrode was electrodeposited through the potentiodynamic method, undergoing only 10 cycles, while maintaining the other parameters constant. Another electrode was prepared using the galvanostatic method, subjecting it to a constant current of 100 mA for 600 s. The same three-electrode cell configuration was employed in both cases. In all cases, the acid concentration was kept at 1 M. Table 1 provides a summary of the

Table 1
Overview of the methodological characteristics of the different PAni/H_2SO_4 electrodes fabricated in this current study.

Electrode	Potentiodynamic Method			
	Potential range (V)	Scan rate (mV/s)	Cycles	[Monomer] (M)
PAni/H_2SO_4 (I)	−0.2 to 0.7	1	10	0.1
PAni/H_2SO_4 (II)	−0.2 to 0.7	1	60	0.1

Electrode	Potentiostatic Method		
	Potential (V)	Duration (s)	[Monomer] (M)
PAni/H_2SO_4 (III)	0.9	600	0.01
PAni/H_2SO_4 (IV)	0.9	600	0.1
PAni/H_2SO_4 (V)	0.9	300	0.1
PAni/H_2SO_4 (VI)	0.9	180	0.1

Electrode	Galvanostatic Method		
	Current (mA)	Duration (s)	[Monomer] (M)
PAni/H_2SO_4 (VII)	100	600	0.01

electrochemical methods used to prepare various PAni/H_2SO_4 electrodes.

2.2.2. Electrode characterization

The polymerized electrodes (potentiodynamic, 60 cycles) were characterized by using cyclic voltammetry (CV) measurements, which were carried out in a three-electrode configuration with an oversized carbon counter electrode, and an Ag/AgCl (3 M KCl) reference electrode. Each electrode was tested in 0.5 M NaCl solution, and in the corresponding sodium salt of the mineral acid used during the polymerization separately (e.g., PAni/HNO_3 electrode tested in 0.5 M NaCl and then in 0.5 M $NaNO_3$). The concentration of the solution was always kept at 0.5 M. The CVs were carried out in a ±1.0 V potential range, at a 1 mV/s scan rate, for 4 cycles. The first CV cycle is excluded from figures for clarity.

The morphology of these electrodes was analyzed using scanning electron microscopy (SEM) on a JAMP-9500F (JEOL) field emission Auger microscope with a primary beam energy of 5 kV at different magnifications. Elemental analysis of the electrodes was also carried out using Auger electron microscopy (AES) to investigate the presence of different elements on the electrode surface.

2.2.3. Desalination

The polymerized electrodes were employed in an asymmetric CDI cell, as illustrated in Fig. 1. Initially, standard batch mode runs were conducted, employing operational parameters similar to those utilized in our previous desalination work [33]. In this setup, two identical reservoirs, each containing 100 mL of a binary salt solution with concentration of 10 mM of each salt, were employed to feed the CDI cell. During the charging step, one reservoir was utilized, and during the discharging step, the other reservoir was used, with manual switching between charging and discharging. Essentially, the salt was removed from the charging reservoir and released into the discharge reservoir. The flow rate was maintained at 30 mL/min. A potential of ±1.0 V was applied to the CDI cell, and the duration of each charging and discharging half cycle was set to 10 min. The batch desalination process was continued for 8 cycles. At the end of every other cycle, samples were extracted from the charge reservoir for ion chromatography analysis.

To study the adsorption behavior of the polymerized electrodes more closely, an extended charge cycle of 60 min was carried out using the same cell assembly as before. First, the CDI cell was allowed to stabilize for 8 charge-discharge cycles undisturbed, i.e., just by switching the potential and keeping the same solution. The charging-discharging potential was set to ±0.35 V. All the experiments were also conducted in 10 mM binary salt solutions, similar to previous desalination runs. The duration of each charge and discharge cycle during stabilization was 1 h. During a new charge cycle, samples were taken at regular intervals to elucidate the adsorption behavior. The first sample was taken before a potential is applied to the cell, which serves as the baseline concentration. Then samples were taken at 1 min, 5 min, 10 min, and then in 10-minute intervals until 60 min in total. The polymer-coated electrodes were compared with pristine carbon electrodes. All these experiments were conducted in triplicate. In addition, all samples were analyzed in analytical triplicates and the average values are reported.

3. Results and discussion

3.1. PAni synthesis and characterization

The cyclic voltammograms (CVs) illustrating the electrodeposition of each PAni system are depicted in Fig. 2. PAni polymerization unfolds through a series of distinct stages [16]. Initially, the aniline monomer undergoes oxidation, leading to the formation of cation radicals. Subsequently, coupling of radicals results in the creation of dimers and oligomers, propelling the polymerization process. Finally, the polymer coating is doped with the anions present in the solution. In Fig. 2A, B, and C, the CVs of the H_2SO_4, HCl, and HNO_3 PAni systems reveal two prominent redox peaks. The first peak, observed between 0 to +0.3 V vs. Ag/AgCl, corresponds to the propagation of polyaniline. The second peak, occurring between +0.3 to +0.6 V vs. Ag/AgCl, is associated with the reversible oxidation of hydroquinone to benzoquinone [29]. In contrast, the CV curve for H_3PO_4 (Fig. 2D), is largely featureless. Although there is a subtle indication of the two redox peaks, their prominence is particularly diminished. This outcome may be attributed to the comparatively less acidic nature of phosphoric acid [19]. In light of this, we have conducted a separate polymerization of aniline in 5 M phosphoric acid, while keeping the other parameters a constant, which yielded the characteristic CV for aniline polymerization (Fig. 2D inset). Nevertheless, we continued the rest of the experiments with 1 M acid concentrations for reasons of comparison. It can also be observed that the curves of PAni/H_2SO_4 (Fig. 2A) and PAni/HNO_3 (Fig. 2C) are similar in magnitude, while PAni/HCl (Fig. 2B) and PAni/H_3PO_4 (Fig. 2D)

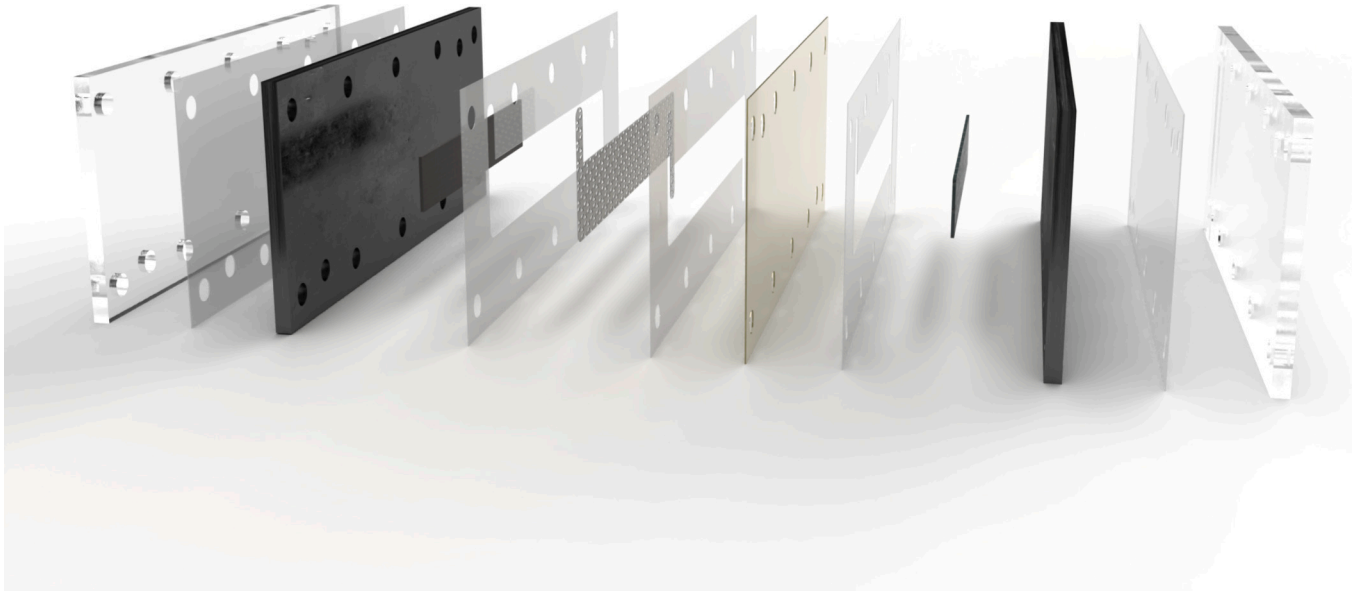

Fig. 1. Schematic of the used asymmetric CDI cell. From left to right, the components are end plate, gasket, current collector, pristine or modified AC electrode, gasket, spacer, gasket, CEM, gasket, carbon cloth counter electrode, current collector, gasket, and end plate.

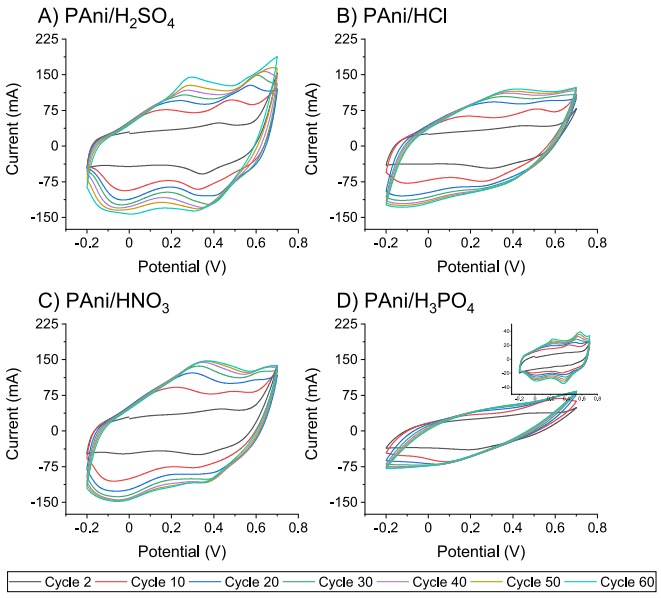

Fig. 2. CV plots generated during the electrodeposition of PAni with A) H_2SO_4, B) HCl, C) HNO_3, and D) H_3PO_4 using the potentiodynamic method with 60 scans at 1 mV/s scan rate, in 1 M acid concentration and 0.1 M aniline concentration (250 mL). The inset in (D) depicts the CV plot from using 5 M phosphoric acid.

exhibit less surface area, which can be indicative of the amount of polymer deposited.

Fig. 3 depicts the electron micrographs of pristine carbon electrode at ×5,000 (A) and ×10,000 (B) and PAni/H_2SO_4 electrode at ×5,000 (C) and ×10,000 (D) magnification. The SEM images illustrate the morphological changes on the surface of the polymerized electrode (Fig. 3C and D) compared to the pristine carbon (Fig. 3A and B). It can also be observed that some of the electrode's macropores are covered, indicating the successful deposition of a polymer coating.

Table S1 summarizes the elemental analysis conducted via AES on both pristine carbon and PAni-coated electrodes. Additionally, Fig. S1 presents the elemental analysis of the PAni/H_2SO_4 electrode. As anticipated, the pristine electrode exhibits solely carbon and oxygen. In contrast, the elemental analysis of the PAni/H_2SO_4 electrode reveals the presence of nitrogen and sulfur, stemming from the polymerization process, alongside carbon and oxygen. This observation serves as supporting evidence affirming the success of the polymerization process. The PAni/HNO_3 electrode shows visually, and chemically similar composition (with the obvious lack of sulfur) as indicated by SEM (Fig. S2) and AES (Table S1) data. The carbon, nitrogen, and oxygen content of the electrode are comparable to that of the PAni/H_2SO_4 electrode. In contrast, the PAni/HCl and PAni/H_3PO_4 electrodes display significantly lower nitrogen content, indicating that the amount of polymer on these electrodes are comparably lower, in line with the surface area of the CV plots (Fig. 2). This can also be visually confirmed by the SEM images (Fig. S2), as they depict a closer resemblance to the pristine electrode. Particularly intriguing are the results from the PAni/H_3PO_4 electrode polymerized in 5 M H_3PO_4. Both SEM (Fig. S2G and H)

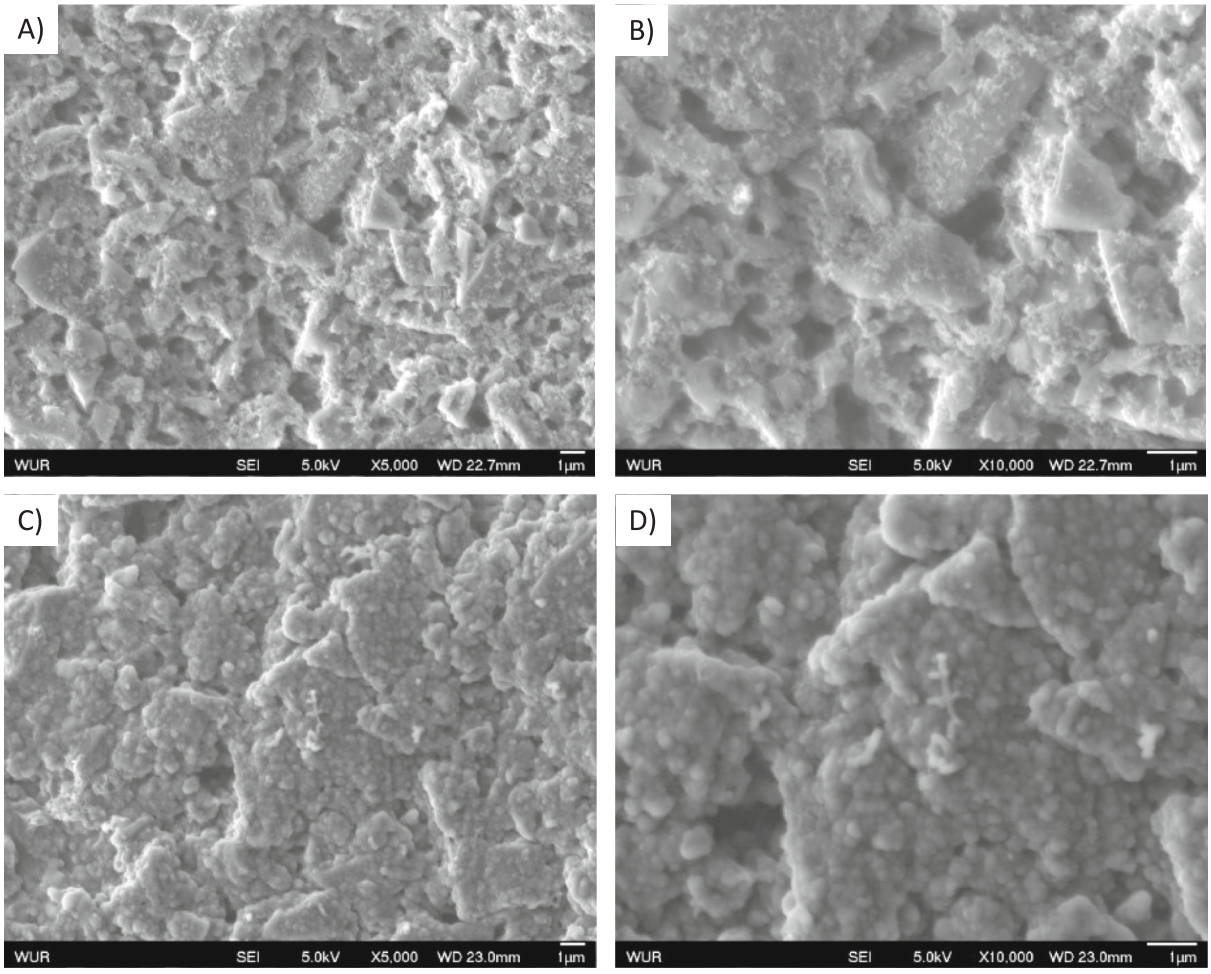

Fig. 3. Scanning electron micrographs of pristine (A, B) and PAni/H_2SO_4 (C, D) electrodes.

and AES (Table S1) data reveal that by increasing the acid concentration to 5 M, the polymerization is comparable to that of PAni/H_2SO_4.

Fig. 4 illustrates the behavior of the fabricated electrodes in comparison with pristine electrodes, across various salt solutions. The pristine electrodes exhibit featureless CV plots, as anticipated, indicating the absence of defined redox processes occurring. Furthermore, these electrodes demonstrate consistent behavior in all tested salts, as evidenced by the CV plots. In contrast, the CV plots of the PAni electrodes reveal distinct redox peaks associated with PAni oxidation and reduction. While there is a noticeable disparity between polymerized and pristine electrodes in general, the PAni electrodes exhibit only marginal variations between different salts. Nevertheless, the PAni/H_2SO_4, PAni/HCl, and PAni/H_3PO_4 electrodes display a greater affinity for sulfate, chloride, and phosphate uptake, respectively. The electrode behavior concerning salt adsorption has been investigated by utilizing several CDI experiments.

3.2. CDI experiments

Fig. 5 provides insights into the initial desalination runs with CDI. The consistent trend across various cases indicates that, on average, the modified electrodes remove a lower quantity of salt compared to the pristine electrode. This phenomenon may be attributed to the reduction in available surface area and pore volume resulting from the electrodeposition of polyaniline, as previously reported in literature [28,29,34]. A more detailed analysis of the results in Fig. 5 reveals intriguing aspects. The pristine carbon electrode exhibits a preference for removing chloride over dihydrogen phosphate and sulfate, except in the presence of nitrate, where the preference shifts towards nitrate ions. Notably, both the PAni/HNO_3 and PAni/HCl electrodes (depicted in Fig. 5A and B, respectively) exhibit similar behavior. These modified electrodes remove a comparable amount of chloride, akin to the pristine electrode, while experiencing a reduction in nitrate removal. In the case of the PAni/HNO_3 electrode, this is contrary to the desired outcome, as ideally, one would expect either a reduction in chloride removal, an increase in nitrate removal, or a combination of both. On the other hand, the PAni/HCl electrode exhibits a step in the desired direction, where the nitrate adsorption is impeded by ~45 % while the chloride adsorption is only reduced by ~24 %. While this observation alone may not conclusively indicate an enhancement in selectivity, it does suggest the potential for further tuning the process to achieve the desired balance in ion removal. In contrast with the pristine electrode, the PAni/H_3PO_4 electrode (Fig. 5C) exhibits reduced chloride adsorption, while the phosphate adsorption is increased slightly during the first 6 cycles. However, the pristine electrode surpasses the PAni/H_3PO_4 electrode in terms of phosphate adsorption by the 8th cycle. In terms of chloride vs. sulfate, the pristine electrode exhibits similar adsorption behavior, with chloride showing slightly higher adsorption. While the PAni/H_2SO_4 electrode (Fig. 5D) still exhibits higher chloride adsorption, the amount of chloride removed is impeded by ~53 % whereas the sulfate adsorption is only impeded by ~16 %. Given this trend, the PAni/H2SO4 was subjected to further studies.

Overall, the initial desalination experiments reveal that there could be a possibility of enhancing the selectivity of CDI electrodes by using PAni doped with different counter ions. To further elucidate the adsorption behavior, the electrodes mentioned in Table 1 were analyzed

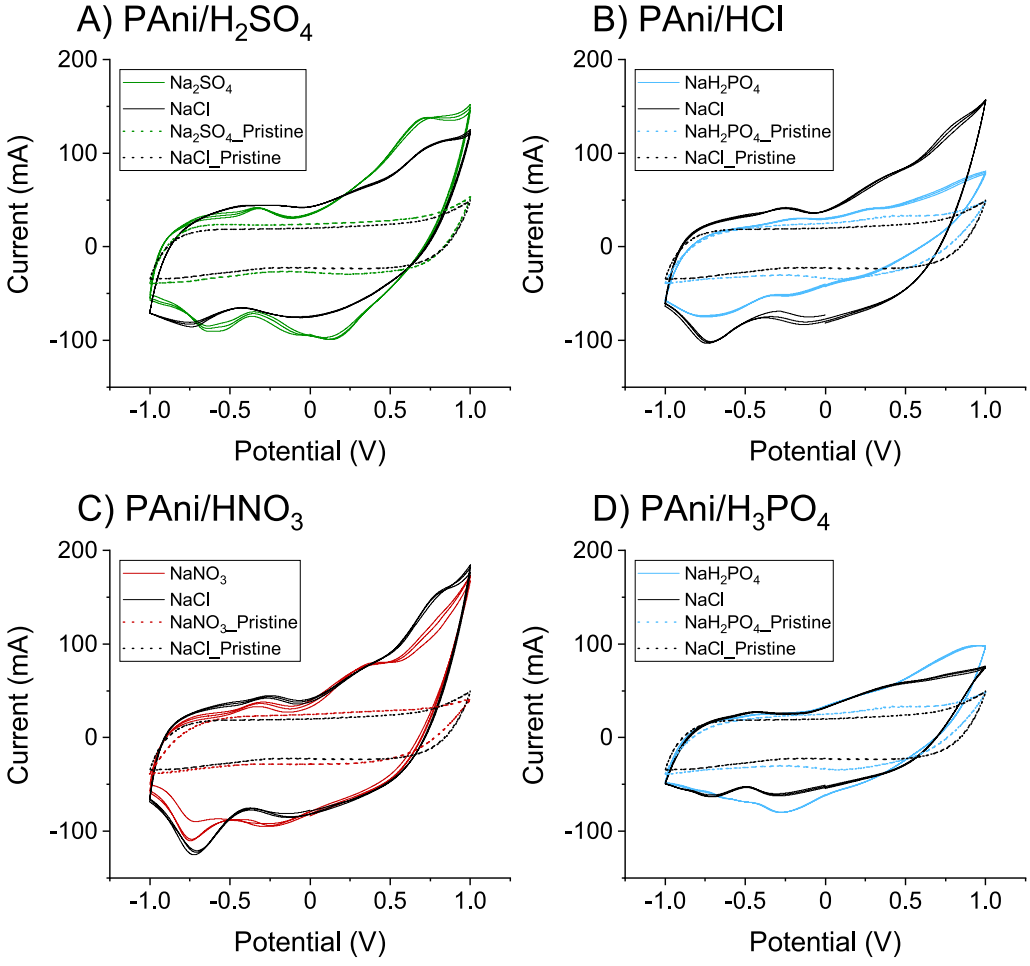

Fig. 4. CVs from PAni electrodes (solid lines) and pristine electrodes (dotted lines) in different electrolytes.

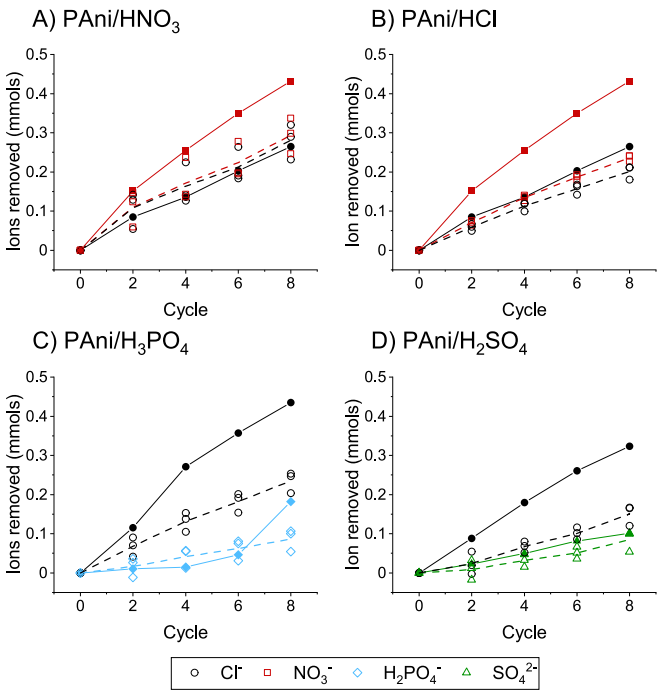

Fig. 5. The quantity (mmols) of each anion removed over 8 cycles of CDI runs, using binary salt solutions, is presented, utilizing both polyaniline-modified electrodes (prepared through the potentiodynamic method with 60 cycles) and pristine carbon electrodes. The data points corresponding to pristine carbon electrodes are represented by closed symbols, while the open symbols depict data from the modified electrodes. Dashed lines on the graph indicate the average values derived from the modified electrodes, providing a visual guide for interpretation.

during longer charge cycles, in 10 mM chloride and sulfate solutions, by sampling in regular intervals.

In contrast with previous desalination experiments (Fig. 5), which involved testing the electrodes through 8 shorter charge-discharge cycles, Fig. 6 presents data from an extended single charge cycle, revealing the varying amounts of each anion removed by the electrode. The

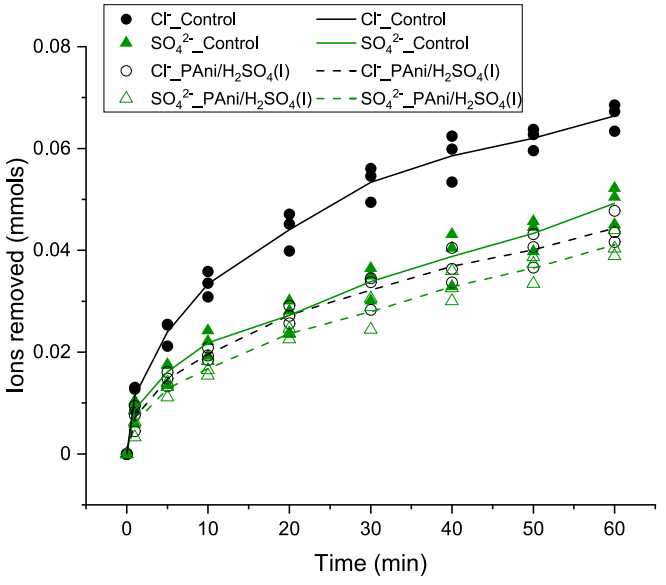

Fig. 6. Cumulative anion adsorption by the pristine carbon (control, solid symbols) and the PAni/H_2SO_4 (I) (open symbols) electrode during a one-hour charge cycle. The lines (average) serve as a guide to the eye.

experimental procedure for all PAni/H_2SO_4 (I)-(VII) electrodes was consistent, and for clarity, the corresponding data is presented in Fig. S3. Fig. 7 summarizes this data, normalized based on the amount of anions removed by the control experiment.

The data presented in Fig. 7 reveals a general trend wherein chloride removal is impeded, while sulfate removal remains virtually unaffected by electrode modifications, except in two cases. Both PAni/H_2SO_4 (I) and (VII) electrodes exhibit a reduction in both chloride (~33 % and ~22 % respectively) and sulfate (~17 % and ~16 % respectively) removal. Conversely, PAni/H_2SO_4 (II) electrode exhibits negligible differences compared to the control. PAni/H_2SO_4 (III)-(VI) demonstrates similar sulfate removal while removing varying amounts of chloride. In light of this, it is worth examining the conditions in which these electrodes were prepared. The electrodes (IV) through (VI) underwent polymerization for 600 s, 300 s, and 180 s respectively, in 0.1 M monomer and 1 M acid solutions. This trend is visualized in Fig. S4. Thus, a shorter polymerization duration corresponds to higher chloride inhibition. In contrast, the PAni/H_2SO_4 (III) electrode was polymerized for 600 s at a lower monomer concentration of 0.01 M while still maintaining the acid concentration at 1 M, which also resulted in lower chloride removal. These results imply the existence of an optimal PAni amount that could promote the electrode's selectivity. Considering these results, the same polymerization conditions of PAni/H_2SO_4 (III) electrode were extended to PAni/HCl, PAni/HNO_3, and PAni/H_3PO_4 electrodes and were tested using CDI under the same conditions. The results from these experiments are presented in Fig. S5 and summarized in Table 2.

The PAni/HCl electrode was tested in both chloride vs. nitrate and chloride vs. phosphate solutions. In the chloride vs. nitrate scenario, there is evidence of hindered nitrate adsorption. Conversely, in the chloride vs. phosphate case, a slight increase in the adsorption of both anions is observed. Notably, both PAni/HNO_3 and PAni/H_3PO_4 electrodes exhibit reduced adsorption in all cases, suggesting that the polymerization conditions do not uniformly impact all tested PAni systems. These findings imply that, under the specified testing parameters, achieving selectivity may involve restricting the adsorption of competing anions rather than increasing the adsorption of the target ions.

3.3. Outlook

The primary focus of this study was to assess the feasibility of utilizing activated carbon electrodes, modified through the polymerization of polyaniline doped with various anions, for their potential in selective ion separation. The polymerization processes were executed in a uniform and straightforward manner, as previously described, for ease of comparison. In light of the observed salt adsorption behaviors of the electrodes, a retrospective analysis is deemed valuable.

The electropolymerization of aniline has been studied by numerous research groups, albeit the studies were predominantly focused on non-porous electrodes [21]. While there is no general consensus on the rate-determining step in electrochemical oxidation of PAni [35], the oxidation of the monomer or their dimerization is commonly considered to be the rate-limiting step in aniline polymerization [36]. Analogous behavior can be observed during chemical polymerization of aniline, where an “induction period” exists before the polymerization proceeds. After the induction period, the reaction can be followed by measuring the temperature increase [36]. An autocatalytic nature characterizes aniline polymerization, wherein fully oxidized polyaniline (pernigraniline) can catalyze the oxidation of aniline monomers while undergoing reduction into emeraldine. This can be observed when the anodic vortex potentials exceed 0.8 V, causing the corresponding anodic peak during the first CV scan shifts to lower potentials in successive scans [37]. Another important facet that affects the rate of aniline polymerization is the available electrode surface area, likely due to the fact that comparatively more aniline monomers can be oxidized at the anode

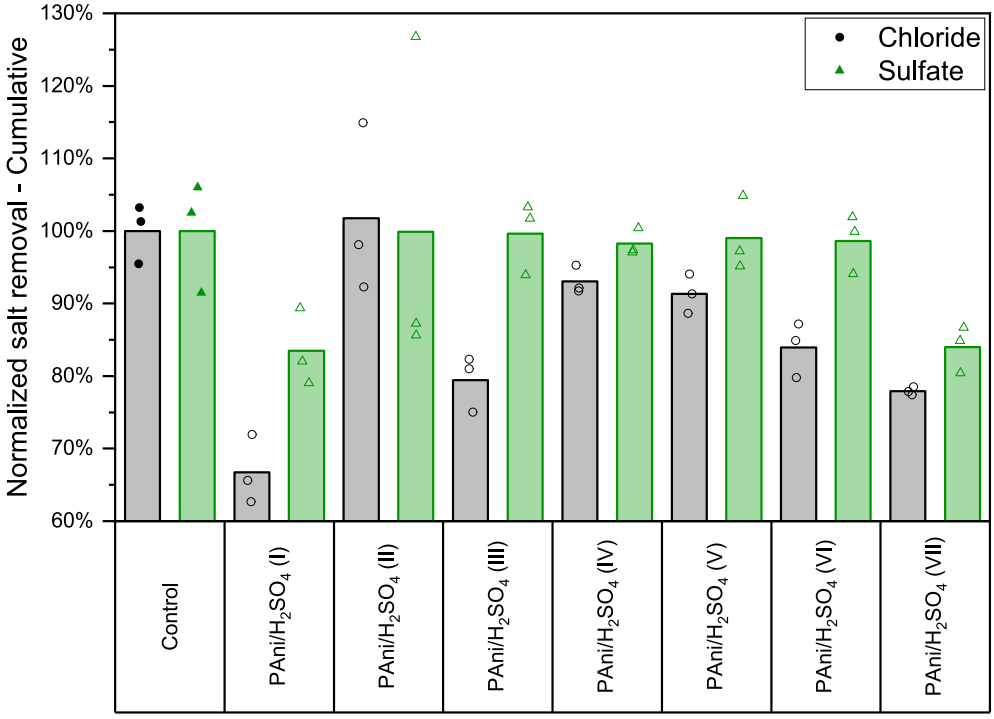

Fig. 7. The percentage of chloride and sulfate removed by respective electrodes normalized by the control. The bars depict the average whereas the symbols represent data from individual experiments.

Table 2
Percentage of each anion (normalized by control) removed by PAni electrodes polymerized using 0.01 M aniline in 1 M acids for 600 s. A negative value indicates a reduction in anion removal compared to the control experiment.

	PAni/HCl		PAni/HNO_3	PAni/H_3PO_4
Chloride	1.5 %	6 %	−7 %	−5 %
Nitrate	−14 %	–	−15 %	–
Phosphate	–	5.0 %	–	−11 %

surface simultaneously. Moreover, similar to that of heterogeneous catalysis, the monomers adsorbed on the surface would undergo changes in their electron density distribution, rendering them more reactive than those in the bulk solution [38]. The polymerization of aniline is a process where the electrode surface is subjected to dynamic changes, with each deposited polymer layer acting as a new surface for any subsequent polymerization step. Therefore, these constant changes on the electrode can also affect the polymerization rate and morphology. Essentially, during a potentiodynamic polymerization of aniline on an electrode surface, redox peaks shift to lower potentials as the polymerization progresses due to these effects [27]. However, the contrary was observed during the modification of activated carbon electrodes as shown in Fig. 2. It can be rationalized that maintaining the anodic vortex potential at 0.7 V during these experiments could limit the full oxidation into pernigraniline minimizing the autocatalytic effect. Moreover, as seen from the CDI experiments, the modified electrodes exhibited reduced salt adsorption compared to pristine electrodes, which was attributed to the reduced available surface area due to the polymer clogging the surface of the electrode. This reduction of the surface area could also affect the rate of polymerization. The CV scans shown in Fig. 2 suggest that the increasing current with each subsequent scan is starting to reach diminishing returns at higher number of cycles. Furthermore, it is evident that the peaks are shifting towards more positive potentials, suggesting that the electrodeposition is becoming increasingly more demanding.

To further unveil the difference in polymerization on a porous surface and a non-porous surface, an additional electrodeposition was conducted on a graphite sheet. This graphite sheet was sourced from the same batch of activated carbon electrodes, simply a piece (7 cm × 2 cm) without any activated carbon material was cut out for this experiment. The polymerization was carried out in the identical conditions as the PAni/H_2SO_4 (II) electrode.

The polymerization of aniline on a graphite substrate reveals several intriguing phenomena. Analysis of the CV scan (Fig. 8A) resulting from the polymerization process indicates a continual increase in current with each successive scan, suggesting that the process has not yet reached a point of diminishing returns, unlike electrodepositions on activated carbon surfaces (Fig. 2). This suggests further potential for the polymerization process to progress. Notably, the shift in peak position observed during successive scans on activated carbon electrodes is minimized here (Fig. 8B), indicating that electrodeposition on activated carbon undergoes more dynamic changes. Fig. 8C and D depict the pristine graphite surface and the surface after polymerization, respectively, showing a globular morphology of the polymer, analogous to the observations on activated carbon electrodes. Numerous factors such as dopants, electrolytes, substrate, and scan rate of the first potential scan influence the morphology and polymerization rate of aniline [26,39–47], as further evidenced by SEM images presented in this study. The morphologies resulting from H_2SO_4 (Fig. 3C and D) and HNO_3 (Fig. S2C and D) appear similar, while films from 5 M H_3PO_4 (Fig. S2G and H) exhibit a more sponge-like structure. Conversely, discernable structures are absent on PAni/HCl and PAni/H_3PO_4 (1 M) electrodes compared to the pristine electrode.

Fig. 8E, F, and G depicts the cross-sections of PAni/HNO_3, PAni/HCl, and PAni/H_2SO_4 respectively, polymerized with 1 M acid concentration and 0.1 M aniline concentration at 0.9 V for 600 s. Here, a very uniform and porous layer of polymer is formed on the graphite substrate. In the case of HNO_3 (Fig. 8E), the morphology reveals slender polymer strands, contrasting with the coral-like structures observed with HCl and H_2SO_4 (Fig. 8F and G). The thickness of the polymer layer remains consistent at around 20–22 μm for both HNO_3 and HCl, while for PAni/H_2SO_4, it is approximately 10–11 μm. Additionally, Fig. S5 provides a visual

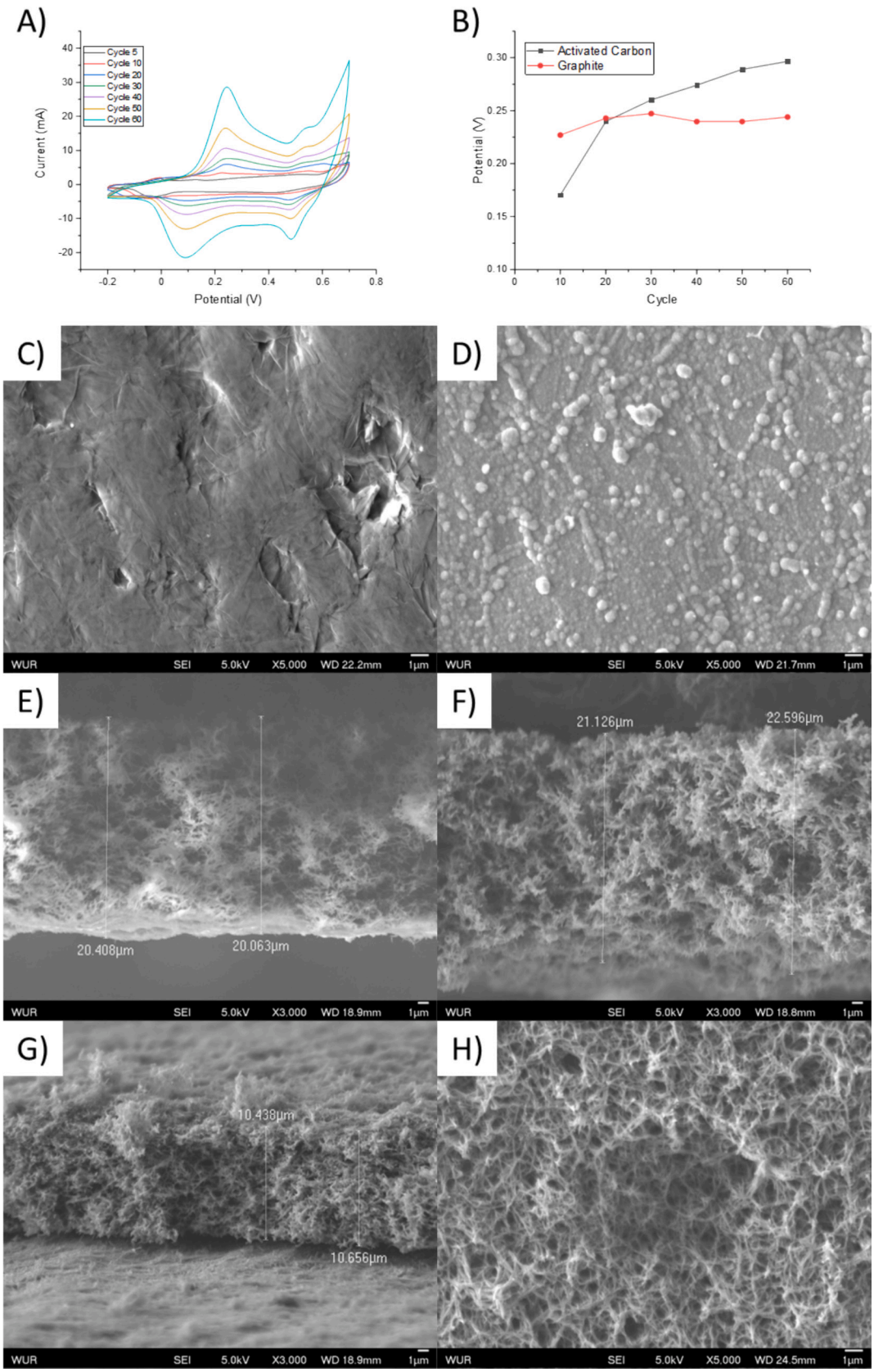

Fig. 8. Aniline polymerization on graphite surface; A) corresponding CV (selected cycles), B) shift in first peak potential during polymerization – activated carbon vs. graphite substrate (the lines serve as a visual guide), Scanning electron micrograph of C) pristine graphite surface, D) graphite surface after polymerization, E), F), and G) cross-sections of PAni/HNO_3, PAni/HCl, and PAni/H_2SO_4 respectively, polymerized with 1 M acid and 0.1 M aniline concentration, at 0.9 V for 600 s. H) top view of (G).

representation of polymer growth over time. No discernible polymer growth was observed at the 60-second mark. However, polymer layers of about 3 μm in thickness were evident after 120 s (Fig. S6A), approximately 6 μm after 180 s, and around 8 μm after 300 s (Fig. S6B). Subsequently, at 420 s (Fig. S6C), the thickness increased to approximately 9 μm, and at 540 s (Fig. S6D), it reached a range of 10–11 μm. Moreover, these images reveal that the morphologies of the polymer network are dependent on the polymerization method. This distinction is particularly visible when comparing Fig. 8D (potentiodynamic) vs. Fig. 8H (potentiostatic). The slow growth of the polymer during the potentiodynamic process results in a dense layer whereas the rapid growth of the polymer during the potentiostatic process results in exceptionally porous structures. Essentially, a higher scan rate during the potentiodynamic polymerization could result in porous PAni structures. The morphology and the thickness of the PAni/H_3PO_4 could unfortunately not be determined, as the polymer layer rinsed off after the polymerization and not retained on the graphite substrate. However, it was observed that a thick layer of polymer, similar to those observed with other systems, is formed on the graphite surface during the polymerization process, especially in the case of 5 M H_3PO_4. The morphology of electrode coatings is pivotal for capacitive ion storage/adsorption mechanisms. While the memory effect of the dopants was not as pronounced within the tested parameters, our results indicate that optimizing polymerization parameters for accessible polyaniline films could offer promising avenues for imparting ion-selective properties on CDI electrodes.

4. Conclusion

This study focused on examining the feasibility of enhancing the ion selective properties of CDI electrodes through modifying the said electrodes with polyaniline coatings doped with various anions. In this endeavor, four mineral acids, namely HCl, HNO_3, H_2SO_4, and H_3PO_4 were used as electrolytes during the electrodeposition stage of the polymer. It was observed that the coated electrodes exhibit reduced total ion adsorption compared to the pristine electrodes. Investigation into polymerization conditions, particularly within the PAni/H_2SO_4 system, revealed restricted chloride adsorption relative to the pristine electrode during extended CDI charge cycles, while sulfate adsorption remained virtually unchanged. This effect was enhanced when the monomer concentration or the polymerization duration was reduced, suggesting the existence of an optimal polymer amount. Consequently, when the electrode was fabricated with a lower aniline concentration of 0.01 M, chloride adsorption was limited by around 20 %. Similarly, with a shortened polymerization duration of 180 s, chloride restriction was approximately 16 %, while maintaining consistent sulfate adsorption levels in both instances. It was further determined that the influence of the dopant anion plays a vital role in the ion adsorption behavior, as evidenced by differing behaviors among PAni systems under identical polymerization conditions, questioning the direct transferability of such conditions. The potentiodynamic polymerization resulted in dense polymer films while the potentiostatic method resulted in porous structures. Varied polymer morphologies were observed based on acid type, concentration, and polymerization method, paving the way for further research to elucidate the impact of polymerization conditions on morphology and subsequent ion adsorption behavior, particularly on porous substrates.

CRediT authorship contribution statement

J.G. Gamaethiralalage: Writing – review & editing, Writing – original draft, Visualization, Methodology, Investigation, Formal analysis, Data curation, Conceptualization. **Jens Muff:** Writing – review & editing, Supervision, Funding acquisition, Formal analysis, Conceptualization. **Louis C.P.M. de Smet:** Writing – review & editing, Supervision, Project administration, Funding acquisition, Formal analysis, Conceptualization.

Funding

This study was supported by the European Research Council (ERC Consolidator Grant 682444, E-motion, PI de Smet) and the Poul Due Jensen Grundfos Foundation as part of the Circular lake restoration – rePair project. Article publishing charges were provided by Dutch Consortium of University Libraries and the National Library of The Netherlands.

Declaration of competing interest

The authors declare the following financial interests/personal relationships which may be considered as potential competing interests: J. G. Gamaethiralalage reports financial support was provided by European Research Council. J. Muff reports financial support was provided by Poul Due Jensen Grundfos Foundation. L.C.P.M. de Smet reports financial support was provided by European Research Council. L.C.P.M. de Smet reports article publishing charges were provided by Dutch Consortium of University Libraries and the National Library of The Netherlands.

Acknowledgments

The authors would like to thank Mr. Hans Beijleveld (WUR), Ms. Dorte Spangsmark, Ms. Linda Birkebæk Madsen, and Mr. Nicolai Nielsen (AAU) for technical support, Dr. Sidharam Pujari (WUR) for assistance with SEM and AES measurements, and Dr. Rudi Nielsen (AAU) for the electrode holder. JGG would like to thank the graduate school VLAG (Biobased, Biomolecular, Chemical, Food, and Nutrition sciences) of Wageningen University for the VLAG research fellowship, and particularly Dr. Jochem Jonkman, Dr. Anouk Geelen, and Ms. Vesna Prsic for their kind support.

Appendix A. Supplementary data

Supplementary data to this article can be found online at https://doi.org/10.1016/j.porgcoat.2024.108854.

Data availability

The data that support the findings of this study are available from the corresponding author on request.

References

[1] J.G. Gamaethiralalage, K. Singh, S. Sahin, J. Yoon, M. Elimelech, M.E. Suss, P. Liang, P.M. Biesheuvel, R.L. Zornitta, L.C.P.M. de Smet, Recent advances in ion selectivity with capacitive deionization, Energy Environ. Sci. 14 (2021) 1095–1120, https://doi.org/10.1039/d0ee03145c.
[2] S. Porada, R. Zhao, A. van Der Wal, V. Presser, P.M. Biesheuvel, Review on the science and technology of water desalination by capacitive deionization, Prog. Mater. Sci. 58 (2013) 1388–1442, https://doi.org/10.1016/j.pmatsci.2013.03.005.
[3] J. Oladunni, J.H. Zain, A. Hai, F. Banat, G. Bharath, E. Alhseinat, A comprehensive review on recently developed carbon based nanocomposites for capacitive deionization: from theory to practice, Sep. Purif. Technol. 207 (2018) 291–320, https://doi.org/10.1016/j.seppur.2018.06.046.
[4] J.E. Dykstra, K.J. Keesman, P.M. Biesheuvel, A. van der Wal, Theory of pH changes in water desalination by capacitive deionization, Water Res. 119 (2017) 178–186, https://doi.org/10.1016/J.WATRES.2017.04.039.
[5] J. Choi, P. Dorji, H.K. Shon, S. Hong, Applications of capacitive deionization: desalination, softening, selective removal, and energy efficiency, Desalination 449 (2019) 118–130, https://doi.org/10.1016/j.desal.2018.10.013.
[6] M.E. Suss, S. Porada, X. Sun, P.M. Biesheuvel, J. Yoon, V. Presser, Water desalination via capacitive deionization: what is it and what can we expect from it? Energy Environ. Sci. 8 (2015) 2296–2319, https://doi.org/10.1039/c5ee00519a.
[7] G. Wulff, Molecular imprinting in cross-linked materials with the aid of molecular templates — a way towards artificial antibodies, Angew. Chem. Int. Ed. Engl. 34 (1995) 1812–1832, https://doi.org/10.1002/anie.199518121.

[8] C. Branger, W. Meouche, A. Margaillan, Recent advances on ion-imprinted polymers, React. Funct. Polym. 73 (2013) 859–875, https://doi.org/10.1016/J.REACTFUNCTPOLYM.2013.03.021.
[9] H. Nishide, J. Deguchi, E. Tsuchida, Selective adsorption of metal ions on crosslinked poly(vinylpyridine) resin prepared with a metal ion as a template, Chem. Lett. 5 (1976) 169–174, https://doi.org/10.1246/cl.1976.169.
[10] B. Jia, W. Zhang, Preparation and application of electrodes in Capacitive Deionization (CDI): A state-of-art review, Nanoscale Research Letters 2016 11:1 11 (2016) 1–25. doi:10.1186/S11671-016-1284-1.
[11] X. Su, T.A. Hatton, Redox-electrodes for selective electrochemical separations, Adv. Colloid Interface Sci. 244 (2017) 6–20, https://doi.org/10.1016/j.cis.2016.09.001.
[12] W. Ji, J. Niu, W. Zhang, X. Li, W. Yan, X. Hao, Z. Wang, An electroactive ion exchange hybrid film with collaboratively-driven ability for electrochemically-mediated selective extraction of chloride ions, Chem. Eng. J. 427 (2022) 130807, https://doi.org/10.1016/J.CEJ.2021.130807.
[13] N. Han, R. Gao, H. Peng, Q. He, Z. Miao, K. Wan, Selective recovery of lithium ions from acidic medium based on capacitive deionization-enhanced imprinted polymers, J. Clean. Prod. 373 (2022) 133773, https://doi.org/10.1016/J.JCLEPRO.2022.133773.
[14] X.R. Wang, X. Wang, H.E. Nian, T. Chen, L. Zhang, S. Song, J.H. Li, Y. Wang, Hierarchical MXene/poly-pyrrole-decorated carbon nanofibers for asymmetrical capacitive deionization, ACS Appl. Mater. Interfaces 14 (2022) 53150–53164, https://doi.org/10.1021/acsami.2c14999.
[15] W.S. Huang, B.D. Humphrey, A.G. MacDiarmid, Polyaniline, a novel conducting polymer. Morphology and chemistry of its oxidation and reduction in aqueous electrolytes, Journal of the Chemical Society, Faraday Transactions 1: Physical Chemistry in Condensed Phases 82 (1986) 2385–2400. doi:10.1039/F1 9868202385.
[16] I. Sapurina, J. Stejskal, The mechanism of the oxidative polymerization of aniline and the formation of supramolecular polyaniline structures, Polym. Int. 57 (2008) 1295–1325, https://doi.org/10.1002/PI.2476.
[17] M. Goyal, K. Singh, N. Bhatnagar, Conductive polymers: a multipurpose material for protecting coating, Prog. Org. Coat. 187 (2024) 108083, https://doi.org/10.1016/J.PORGCOAT.2023.108083.
[18] N.V. Blinova, J. Stejskal, M. Trchová, J. Prokeš, M. Omastová, Polyaniline and polypyrrole: a comparative study of the preparation, Eur. Polym. J. 43 (2007) 2331–2341, https://doi.org/10.1016/J.EURPOLYMJ.2007.03.045.
[19] I. Šeděnková, M. Trchová, N.V. Blinova, J. Stejskal, In-situ polymerized polyaniline films, Preparation in solutions of hydrochloric, sulfuric, or phosphoric acid, Thin Solid Films 515 (2006) 1640–1646, https://doi.org/10.1016/J.TSF.2006.05.038.
[20] G. Boara, M. Sparpaglione, Synthesis of polyanilines with high electrical conductivity, Synth. Met. 72 (1995) 135–140, https://doi.org/10.1016/0379-6779(94)02337-X.
[21] J. Stejskal, I. Sapurina, M. Trchová, Polyaniline nanostructures and the role of aniline oligomers in their formation, Prog. Polym. Sci. 35 (2010) 1420–1481, https://doi.org/10.1016/J.PROGPOLYMSCI.2010.07.006.
[22] J. Stejskal, P. Kratochvíl, A.D. Jenkins, The formation of polyaniline and the nature of its structures, Polymer 37 (1996) 367–369, https://doi.org/10.1016/0032-3861(96)81113-X.
[23] H. Okamoto, M. Okamoto, T. Kotaka, Structure development in polyaniline films during electrochemical polymerization. II: structure and properties of polyaniline films prepared via electrochemical polymerization, Polymer 39 (1998) 4359–4367, https://doi.org/10.1016/S0032-3861(97)10105-7.
[24] H. Okamoto, T. Kotaka, Structure and properties of polyaniline films prepared via electrochemical poly-merization. I: effect of pH in electrochemical polymerization media on the primary structure and acid dissociation constant of product polyaniline films, Polymer 39 (1998) 4349–4358, https://doi.org/10.1016/S0032-3861(98)00013-5.
[25] N.V. Blinova, J. Stejskal, M. Trchová, J. Prokeš, Polyaniline prepared in solutions of phosphoric acid: powders, thin films, and colloidal dispersions, Polymer 47 (2006) 42–48, https://doi.org/10.1016/J.POLYMER.2005.10.145.
[26] G. Zotti, S. Cattarin, N. Comisso, Cyclic potential sweep electropolymerization of aniline: the role of anions in the polymerization mechanism, J. Electroanal. Chem. Interfacial Electrochem. 239 (1988) 387–396, https://doi.org/10.1016/0022-0728(88)80293-6.
[27] A. Korent, K.Ž. Soderžnik, S. Šturm, K.Ž. Rožman, A correlative study of polyaniline Electropolymerization and its electrochromic behavior, J. Electrochem. Soc. 167 (2020) 106504, https://doi.org/10.1149/1945-7111/AB9929.
[28] J.C. Wu, S.S. Chen, T.C. Yu, K.C.W. Wu, C.H. Hou, Effective electrochemically controlled removal of fluoride ions using electrodeposited polyaniline-carbon nanotube composite electrodes, Sep. Purif. Technol. 254 (2021) 117561, https://doi.org/10.1016/j.seppur.2020.117561.
[29] R.L. Zornitta, L.A.M. Ruotolo, L.C.P.M. de Smet, High-performance carbon electrodes modified with polyaniline for stable and selective anion separation, Sep. Purif. Technol. 290 (2022) 120807, https://doi.org/10.1016/J.SEPPUR.2022.120807.
[30] F. Gao, X. Li, W. Shi, Z. Wang, Highly selective recovery of phosphorus from wastewater via capacitive deionization enabled by ferrocene-polyaniline-functionalized carbon nanotube electrodes, ACS Appl. Mater. Interfaces 14 (2022) 31962–31972, https://doi.org/10.1021/acsami.2c06248.
[31] C. Li, B. Liu, D. Fang, P. Zhang, F. Li, X. Qiu, X. Mo, K. Li, Polyaniline-derived mesoporous carbon electrode for selective and efficient ammonium removal with in a flow-electrode capacitive deionization system, J. Environ. Chem. Eng. 11 (2023) 110857, https://doi.org/10.1016/J.JECE.2023.110857.
[32] M. Łapkowski, E. Vieil, Control of polyaniline electroactivity by ion size exclusion, Synth. Met. 109 (2000) 199–201, https://doi.org/10.1016/S0379-6779(99)00237-4.
[33] J.G. Gamaethiralalage, L.C.P.M. de Smet, Rocking-chair capacitive deionization for phosphate recovery via rejection mode using ion-exchange membranes, Desalination 564 (2023) 116752, https://doi.org/10.1016/J.DESAL.2023.116752.
[34] X. Feng, G. Yang, Y. Liu, W. Hou, J.J. Zhu, Synthesis of polyaniline/MCM-41 composite through surface polymerization of aniline, J. Appl. Polym. Sci. 101 (2006) 2088–2094, https://doi.org/10.1002/APP.23836.
[35] M. Kalaji, L. Nyholm, L.M. Peter, A microelectrode study of the influence of pH and solution composition on the electrochemical behaviour of polyaniline films, J. Electroanal. Chem. Interfacial Electrochem. 313 (1991) 271–289, https://doi.org/10.1016/0022-0728(91)85185-R.
[36] I.Y. Sapuria, M.A. Shisho, Oxidative polymerization of aniline: Molecular synthesis of polyaniline and the formation of supramolecular structures, in: A.d.S. Gomes (Ed.), New Polymers for Special Applications, IntechOpen, 2012: pp. 251–312. doi:10.5772/3345.
[37] S. Mu, J. Kan, Evidence for the autocatalytic polymerization of aniline, Electrochim. Acta 41 (1996) 1593–1599, https://doi.org/10.1016/0013-4686(95)00410-6.
[38] S. Fedorova, J. Stejskal, Surface and precipitation polymerization of aniline, Langmuir 18 (2002) 5630–5632, https://doi.org/10.1021/la025665o.
[39] H. Tang, A. Kitani, M. Shiotani, Effects of anions on electrochemical formation and overoxidation of polyaniline, Electrochim. Acta 41 (1996) 1561–1567, https://doi.org/10.1016/0013-4686(95)00408-4.
[40] R. Córdova, M.A. del Valle, A. Arratia, H. Gómez, R. Schrebler, Effect of anions on the nucleation and growth mechanism of polyaniline, J. Electroanal. Chem. 377 (1994) 75–83, https://doi.org/10.1016/0022-0728(94)03425-7.
[41] L.J. Duić, Z. Mandić, F. Kovačiček, The effect of supporting electrolyte on the electrochemical synthesis, morphology, and conductivity of polyaniline, J. Polym. Sci. A Polym. Chem. 32 (1994) 105–111, https://doi.org/10.1002/POLA.1994.080320112.
[42] B. Wang, J. Tang, F. Wang, The effect of anions of supporting electrolyte on the electrochemical polymerization of aniline and the properties of polyaniline, Synth. Met. 13 (1986) 329–334, https://doi.org/10.1016/0379-6779(86)90194-3.
[43] L. Dui, S. Grigi, The effect of polyaniline morphology on hydroquinone/quinone redox reaction, Electrochim. Acta 46 (2001) 2795–2803, https://doi.org/10.1016/S0013-4686(01)00491-1.
[44] L. Duić, S. Grigić, The influence of aniline-monomer and sulphuric acid concentrations on the morphology of polyaniline film, Polimeri 18 (1997) 176–180.
[45] T. Boschi, G. Montesperelli, P. Nunziante, G. Pistoia, P. Fiordiponti, Some aspects of the electrochemical growth of polyaniline films, Solid State Ion. 31 (1989) 281–286, https://doi.org/10.1016/0167-2738(89)90467-0.
[46] G.D.T. Andrade, M.J. Aguirre, S.R. Biaggio, Influence of the first potential scan on the morphology and electrical properties of potentiodynamically grown polyaniline films, Electrochim. Acta 44 (1998) 633–642, https://doi.org/10.1016/S0013-4686(98)00185-6.
[47] F. Ziaeimoghaddam, R. Arefinia, Investigation of the effect of doping/dedoping on the redox behavior of polyaniline film: experimental and modeling approach, Prog. Org. Coat. 170 (2022) 106952, https://doi.org/10.1016/J.PORGCOAT.2022.106952.